FULL PAPER

Dalton
www.rsc.org/dalton

Antisymmetric exchange in two tricopper(II) complexes containing a $[Cu_3(\mu_3\text{-}OMe)]^{5+}$ core

Xiaoming Liu,[a] Marcelo P. de Miranda,[a] Eric J. L. McInnes,[b] Colin A. Kilner[a] and Malcolm A. Halcrow*[a]

[a] *Department of Chemistry, University of Leeds, Woodhouse Lane, Leeds, UK LS2 9JT. E-mail: M.A.Halcrow@chem.leeds.ac.uk*

[b] *EPSRC CW EPR Service, Department of Chemistry, University of Manchester, Oxford Road, Manchester, UK M13 9PL*

Received 26th September 2003, Accepted 27th October 2003
First published as an Advance Article on the web 14th November 2003

Reaction of CuX_2 ($X^- = Cl^-$ or Br^-) with 2 molar equivalents of 3{5}-(2,4,6-trimethylphenyl)pyrazole (Hpz^{Mes}) in MeOH in the presence of NaOH yields $[Cu_3X(Hpz^{Mes})_2(\mu\text{-}pz^{Mes})_3(\mu_3\text{-}OMe)]X$ ($X^- = Cl^-$ or Br^-). Crystal structures of these compounds show almost identical triangles of Cu(II) ions, centred by a triply bridging methoxide ligand and with three edge-bridging pyrazolide groups. The mesityl substituents on the bridging pyrazolide ligands are arranged in HT, HH, TT fashion. $\chi_M T$ for both compounds decreases steadily with decreasing temperature, reaching 0.40 cm^3 mol^{-1} K at 70 K before decreasing further below 40 K. This low temperature behaviour could not be interpreted using conventional superexchange Hamiltonians, but was reproduced by an alternative model that incorporated an additional antisymmetric exchange term. This interpretation was confirmed by the Q-band EPR spectra of the two compounds. NMR experiments show that the structures of these compounds are not retained in solution, in contrast to other closely related tricopper compounds. These are the first examples of triangular Cu(II) compounds bearing a $[Cu_3(\mu_3\text{-}OR)]^{5+}$ ($R \neq H$) core motif, and the first triangular compounds showing antisymmetric exchange to have been analysed by both susceptibility and EPR measurements.

Introduction

We have recently described the synthesis of the novel heptacopper complex $[\{Cu_3(Hpz^{tBu})_6(\mu_3\text{-}Cl)(\mu_3\text{-}OH)_3\}_2Cu]Cl_6$ (Hpz^{tBu} = 5-*tert*-butylpyrazole), by reaction of $CuCl_2$ with Hpz^{tBu} in basic MeOH.[1] This compound possesses an unusual $[Cu_7(\mu_3\text{-}OH)_6(\mu_3\text{-}Cl)_2]^{6+}$ vertex-shared double cubane core, which is templated by supramolecular hydrogen-bonding interactions between the non-coordinated Cl^- anions, and the Hpz^{tBu} NH groups and OH^- ligands. We were interested to examine how the steric properties of the pyrazole ligand substituents affect the products obtained from this complexation reaction. We report here that analogous reactions employing 3{5}-(2,4,6-trimethylphenyl)pyrazole (Hpz^{Mes}) afford the very different products, $[Cu_3X(Hpz^{Mes})_2(\mu\text{-}pz^{Mes})_3(\mu_3\text{-}OMe)]X$ (X^- = Cl^-, **1**; X^- = Br^-, **2**). These are the first crystallographically authenticated tricopper complexes to contain a $[Cu_3(\mu_3\text{-}OR)]^{5+}$ ($R \neq H$) core motif. Related compounds containing a $[Cu_3(\mu\text{-}L)_3(\mu_3\text{-}OH)]^{2+}$ core with diatomic L^- bridges have been previously published, where L^- is a pyrazolide,[2–5] triazolide,[6–8] oximate[9–13] or ketonate[14,15] derivative. Complexes **1** and **2** exhibit magnetochemical and EPR spectroscopic properties that can only be interpreted by taking into account antisymmetric exchange, which leads to spin canting within the molecular spin manifold. We have analysed this in some detail.

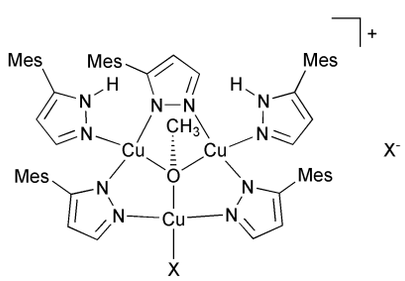

X = Cl, **1**
X = Br, **2**

Results and discussion

A mixture of CuX_2 ($X^- = Cl^-$ or Br^-) and Hpz^{Mes} [16] in a 1 : 2 molar ratio, in MeOH containing excess NaOH, affords a green precipitate after stirring at 290 K for 16 h. Recrystallisation of the filtered solid from CH_2Cl_2 : pentane yields green, crystalline **1** and **2** in yields of 40–60%. The blue filtrate from the reaction mixtures contains a mixture of $[CuX_2(Hpz^{Mes})_4]$ and $[Cu_4(\mu_4\text{-}O)(\mu\text{-}X)_6(Hpz^{Mes})_4]$.[17] Isolated **1** and **2** barely dissolve in chlorinated solvents, but are moderately soluble in MeCN and dmso.

Crystals of **1** and **2** are not isomorphous, despite the almost identical molecular structures exhibited by the two compounds. The complexes consist of a triangle of tetragonal Cu(II) ions, each linked by a doubly-bridging $[pz^{Mes}]^-$ ligand and a central, triply-bridging methoxide ligand (Fig. 1, Table 1). The basal

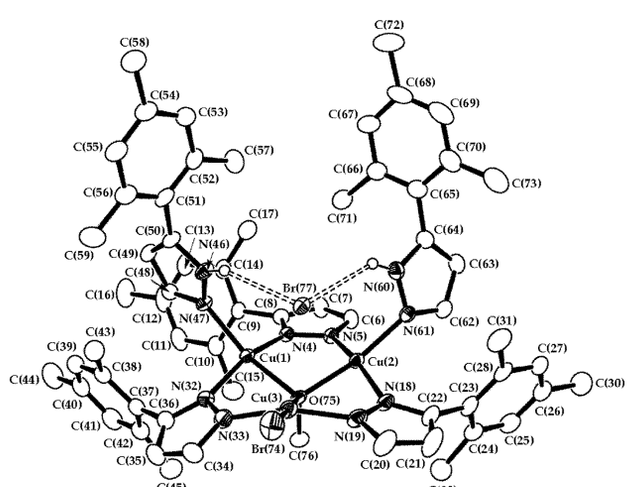

Fig. 1 View of the complex molecule in the crystal structure of **2**, showing the atom numbering scheme employed. Thermal ellipsoids are at the 50% probability level. The molecular structure of **1** is visually almost indistinguishable from that of **2**, and uses an identical atom numbering scheme but with Br(74) and Br(77) replaced by Cl(74) and Cl(77).

DOI: 10.1039/b311980g

Table 1 Selected bond lengths (Å) and angles (°) for **1** and **2**

	1 (X = Cl)	**2** (X = Br)
Cu(1)–N(4)	1.961(3)	1.965(2)
Cu(1)–N(32)	1.960(3)	1.962(3)
Cu(1)–N(47)	1.990(3)	1.999(3)
Cu(1)–O(75)	2.012(3)	2.021(2)
Cu(1)–X(77)	2.9221(8)	3.1011(5)
Cu(2)–N(5)	1.941(3)	1.948(3)
Cu(2)–N(18)	1.940(3)	1.945(3)
Cu(2)–N(61)	2.012(3)	2.012(3)
Cu(2)–O(75)	2.022(3)	2.011(2)
Cu(2)–X(77)	2.7951(9)	2.8772(5)
Cu(3)–N(19)	1.960(3)	1.944(3)
Cu(3)–N(33)	1.953(3)	1.939(3)
Cu(3)–X(74)	2.2470(10)	2.4030(5)
Cu(3)–O(75)	2.099(2)	2.092(2)
Cu(3)–X(77)	2.6896(9)	2.9428(5)
Cu(1) ··· Cu(2)	3.2172(5)	3.2497(5)
Cu(1) ··· Cu(3)	3.2640(6)	3.2551(5)
Cu(2) ··· Cu(3)	3.2001(5)	3.2425(5)
N(4)–Cu(1)–N(32)	161.77(13)	157.60(11)
N(4)–Cu(1)–N(47)	95.93(12)	97.23(11)
N(4)–Cu(1)–O(75)	88.57(11)	87.77(9)
N(4)–Cu(1)–X(77)	98.25(10)	94.74(7)
N(32)–Cu(1)–N(47)	94.81(13)	96.15(11)
N(32)–Cu(1)–O(75)	86.72(11)	85.98(10)
N(32)–Cu(1)–X(77)	96.72(9)	103.55(8)
N(47)–Cu(1)–O(75)	158.75(11)	159.37(9)
N(47)–Cu(1)–X(77)	88.45(9)	88.29(7)
O(75)–Cu(1)–X(77)	70.33(7)	71.31(6)
N(5)–Cu(2)–N(18)	161.69(14)	163.81(11)
N(5)–Cu(2)–N(61)	90.07(14)	89.86(10)
N(5)–Cu(2)–O(75)	88.03(13)	86.81(9)
N(5)–Cu(2)–X(77)	97.72(9)	97.24(8)
N(18)–Cu(2)–N(61)	98.54(12)	97.59(11)
N(18)–Cu(2)–O(75)	88.13(11)	88.17(10)
N(18)–Cu(2)–X(77)	98.28(9)	96.58(8)
N(61)–Cu(2)–O(75)	163.45(11)	169.60(10)
N(61)–Cu(2)–X(77)	90.82(9)	93.85(8)
O(75)–Cu(2)–X(77)	73.17(7)	76.83(6)
N(19)–Cu(3)–N(33)	162.55(13)	160.93(12)
N(19)–Cu(3)–X(74)	93.52(9)	95.22(8)
N(19)–Cu(3)–O(75)	86.75(11)	87.08(10)
N(19)–Cu(3)–X(77)	96.70(9)	90.55(9)
N(33)–Cu(3)–X(74)	93.55(9)	93.15(8)
N(33)–Cu(3)–O(75)	85.54(11)	84.28(9)
N(33)–Cu(3)–X(77)	96.30(9)	103.34(9)
X(74)–Cu(3)–O(75)	177.60(8)	177.37(6)
X(74)–Cu(3)–X(77)	107.79(4)	107.021(18)
O(75)–Cu(3)–X(77)	74.54(7)	74.20(5)
Cu(1)–(O75)–Cu(2)	105.77(11)	107.43(9)
Cu(1)–(O75)–Cu(3)	105.09(10)	104.61(9)
Cu(2)–(O75)–Cu(3)	101.87(10)	104.40(9)

plane of Cu(1) and Cu(2) is completed by a terminal Hpz^{Mes} ligand, while Cu(3) possesses a monodentate X^- (X^- = Cl^- or Br^-) ligand in this position. One apical position of all 3 Cu ions is occupied by a second X^- anion X(77), with long Cu–X(77) distances that suggest only a weak electrostatic bonding interaction to this ligand (Table 1). X(77) also accepts hydrogen bonds from the NH groups of the two Hpz^{Mes} ligands (Fig. 1). The 'τ' index of Addison and Reedijk for Cu(1) and Cu(2) is ≤0.10, close to the ideal value of 0 for an ideal square pyramidal complex;[18] τ for Cu(3) is 0.25 for **1** and 0.27 for **2**, showing that these atoms have a more twisted coordination geometry. The mesityl groups of the bridging $[pz^{Mes}]^-$ ligands have a HT, HH, TT (H = head, T = tail) disposition, which brings two of the mesityl substituents into close proximity so that the methyl groups C(16) and C(44), and C(15) and C(45), are in van der Waals contact with C ··· C ≤ 3.892(6) Å. This structure presumably avoids unfavourable steric repulsions between X(74) and one of the mesityl groups [C(23)–C(31)] or [C(37)–C(45)], which would exist under a HT,HT,HT arrangement.

Each individual Cu–N and Cu–O bond length is equal in the two molecules to within 4 s.u.s (Table 1). The bond angles at Cu [excepting those to X(77)] show slightly more variation, notably N(61)–Cu(2)–O(75) which is 6.15(15)° greater in **2** compared to **1**. This probably reflects the different positions of the X(77) anion, which is hydrogen-bonded to N(60), in the two structures; Cl(77) in **1** lies closer to Cu(3) than to the other two Cu ions, while Br(77) in **2** occupies a position closest to Cu(2) (Table 1). Both **1** and **2** show an isosceles pattern of Cu–O(75)–Cu angles although, interestingly, the distribution of these angles within the $[Cu_3(\mu_3\text{-OMe})]^{3+}$ triangle is different in the two compounds (Table 1). For **1**, the Cu–O–Cu angles have a 'two large + one small' pattern, with the small angle Cu(2)–O(75)–Cu(3) being adjacent to the chemically unique metal ion Cu(3). In contrast, **2** shows a 'one large + two small' distribution of Cu–O–Cu angles, with the large angle Cu(1)–O(75)–Cu(2) being opposite to Cu(3). Hence, overall the $[Cu_3(\mu_3\text{-OMe})]^{3+}$ core in **1** should show rhombic magnetic symmetry, while in **2** it is axial to within experimental error if the mesityl substituents are ignored. These small differences may have a bearing on the significantly different magnetic and EPR properties shown by **1** and **2** (see below).

Neighbouring molecules in **1** and **2** interact with each other through van-der-Waals contacts only, and the tricopper cores in neighbouring molecules are well-separated from each other. The shortest intermolecular Cu ··· Cu distance in each structure is Cu(1) ··· Cu(3^{i}) = 9.0559(6) Å for **1** (symmetry code i: x, $1 + y$, z) and Cu(2) ··· Cu(3^{ii}) = 9.2581(5) Å for **2** (symmetry code ii: $-\frac{1}{2} + x$, $\frac{3}{2} - y$, z). This means that intermolecular dipolar interactions, and weak intermolecular superexchange, are unlikely to significantly contaminate the magnetochemistry of either compound.

At 300 K, $\chi_M T$ for both **1** and **2** is 0.79 $cm^3\ mol^{-1}$ K, which is smaller than the value of 1.3 $cm^3\ mol^{-1}$ K expected for three non-interacting Cu(II) ions with a reasonable g-value.[19] Upon cooling both samples $\chi_M T$ decreases continuously, plateauing at 0.37–0.40 $cm^3\ mol^{-1}$ K between 40–70 K before decreasing further at lower temperatures (Fig. 2). This 'plateau' value is close to the value of $\chi_M T$ = 0.4 $cm^3\ mol^{-1}$ K expected for an isolated $S = \frac{1}{2}$ ground state with a reasonable g-value for interacting Cu(II) centres.[19] It is noteworthy that the magnetic data for **1** and **2** are very similar above 70 K, but differ significantly below this temperature. The data were first analysed according to a C_3-symmetric Hamiltonian (eqn. (1)).

$$H = -2J\left(S_1 \cdot S_2 + S_1 \cdot S_3 + S_2 \cdot S_3\right) \qquad (1)$$

This can be solved by vector coupling[20] to give eqn. (2), where N, g, β and k have their usual meanings.

$$\chi_M = \left(\frac{Ng^2\beta^2}{4k\left[T-\theta\right]}\right)\left(\frac{1+5\exp\left[3J/kT\right]}{1+3\exp\left[3J/kT\right]}\right) \qquad (2)$$

Fitting the susceptibility curves for **1** and **2** to eqn. (2) yielded the following parameters (Fig. 2): for **1**, g = 2.19, $J = -100\ cm^{-1}$, $\theta = -9.0$ K; for **2**, g = 2.20, $J = -103\ cm^{-1}$, $\theta = -8.5$ K. Unfortunately, even with the incorporation of a Weiss constant ('θ') into this analysis to take account of the low-temperature behavior, the data below 40 K were not well reproduced by this model (Fig. 2). Alternative analyses using a C_2-symmetric model derived from eqn. (3), to take account of the slightly 'isosceles' Cu–O–Cu angles in **1** and **2**, did not result in improved fits and gave highly correlated J and J' values that could not be refined unambiguously.[3,7,8]

$$H = -2J\left(S_1 \cdot S_2 + S_1 \cdot S_3\right) - 2J'\left(S_2 \cdot S_3\right) \qquad (3)$$

The low-temperature decline in $\chi_M T$ to a value smaller than that for 1 unpaired electron has been observed in all magneto-

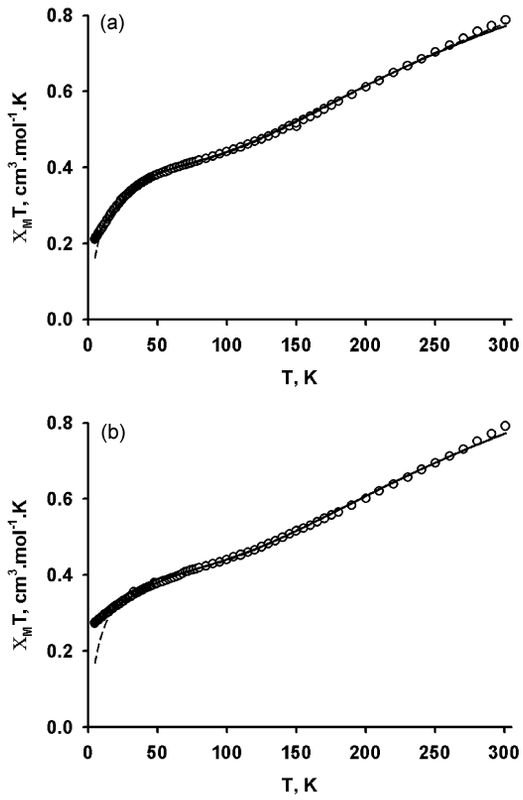

Fig. 2 Plot of $\chi_M T$ *vs.* T (circles) for powder samples of **1** (top) and **2** (bottom). The dashed lines show the best theoretical fit of the data to eqn. (2), while the solid lines show the best theoretical fits obtained from eqns. (4)–(9). See text for fitting details.

chemical studies of $[Cu_3(\mu_3\text{-OH})]^{5+}$ [3,4,8,13,14,21] and $[Cu_3(\mu_3\text{-O})]^{4+}$ [5] complexes except one,[15] and arises from intramolecular antisymmetric exchange between the two near-degenerate $S = ½$ states.[8,21] Antisymmetric exchange in this system is a second-order perturbation caused by the effects of spin–orbit coupling on the exchange interaction. The antisymmetric exchange term, which tends to align spins perpendicular to each other, competes with the spin-(anti)parallel alignment imposed by symmetric (anti)ferromagnetic exchange. This results in canting of the individual Cu spins within the molecule, so that the *net* magnetic moment shown by the individual, antisymmetrically coupled spin states no longer corresponds to a simple multiple of one unpaired electron. This results in a corresponding perturbation of the two lowest-lying spin-state energies levels in the molecule (Scheme 1).[8]

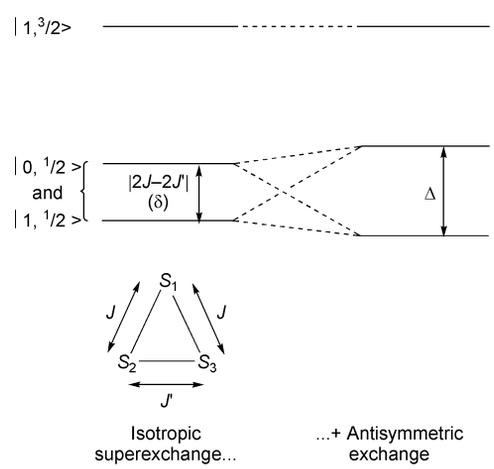

Scheme 1 Perturbation of the spin energy levels $|S_A, S_T>$ ($S_A = S_2 + S_3$; $S_T = S_1 + S_A$) of a C_{2v}-symmetric triangle of $S = ½$ spins (eqn. (3)), caused by the incorporation of antisymmetric exchange (eqn. (4)). † The symbols denoting the gaps between energy levels are defined in the text.

Antisymmetric exchange can be incorporated into the magnetochemical analysis of **1** and **2** using the following Hamiltonian for a triangle of Cu(II) spins (eqn. (4)):[8,21–23]

$$H = -2J(S_1 \cdot S_2 + S_1 \cdot S_3) - 2J'(S_2 \cdot S_3) + \boldsymbol{G}([S_1 \times S_2] + [S_2 \times S_3] + [S_3 \times S_1]) \quad (4)$$

where $\boldsymbol{G}$ is the antisymmetric exchange vector.[21,22] Diagonalisation of this Hamiltonian leads to analytical expressions for the energies of the three unique spin levels in the molecule with energies $E\{S_A, S_T\}$ ($S_A = S_2 + S_3$; $S_T = S_1 + S_A$; Scheme 1), given by eqns. (5)–(9):

$$E\left\{1, \tfrac{1}{2}\right\} = J + \frac{J'}{2} - \frac{\Delta}{2} \quad (5)$$

$$E\left\{0, \tfrac{1}{2}\right\} = J + \frac{J'}{2} + \frac{\Delta}{2} \quad (6)$$

$$E\left\{1, \tfrac{3}{2}\right\} = -J - \frac{J'}{2} \quad (7)$$

$$\delta = \left|-2J - 2J'\right| \quad (8)$$

$$\Delta^2 = \delta^2 + 3G^2 \quad (9)$$

This shows that only the energies of the two $S = ½$ spin states are perturbed by the antisymmetric exchange constant G (Scheme 1). †

To fit the experimental data, theoretical susceptibilities were calculated by a perturbation treatment of the eigenstates obtained from the diagonalisation of eqn. (4). The non-vanishing components of the susceptibility tensor were then calculated according to a generalised susceptibility equation. ‡[24] Importantly, it was necessary to consider the parallel and perpendicular susceptibility components separately, since these are afffected differently by the $\boldsymbol{G}$ vector. In principle, fitting the susceptibility data to this axially symmetric model requires six independent variables. However, examination of the correlations between these parameters allowed us to make the following simplifications.

First, the different components of $\boldsymbol{G}$ (G_z and G_{xy} in axial symmetry) were strongly correlated with each other when allowed to refine independently; only the modulus of the $\boldsymbol{G}$ vector was well-defined by the data. Hence, in the final model it was assumed that the components of $\boldsymbol{G}$ follow the relation $G_z >> G_x, G_y \approx 0$. This approximation is valid for a weakly axial system with $J \approx J'$,[22] and has been used by others to model antisymmetric exchange in trinuclear complexes.[8,21] The effective antisymmetric exchange constant G is then equal to $3^{½}G_z/6$.[23] Importantly, the sign of G is also undefined under these

† While the G values reported for the two compounds in ref. 8 are correct, the resultant energy levels were calculated using a Hamiltonian, in which the $(S_3 \times S_1)$ term in eqn. (4) was replaced by $(S_1 \times S_3)$. This breaks the permutation symmetry of the Hamiltonian,[23] and unfortunately leads to erroneous results.[43] The correct equations for the energy levels derived from the susceptibility analysis in this type of system are given in eqns. (5)–(9) and Scheme 1.

‡ The commonly-used form of the van Vleck equation in eqn. (14) cannot be employed in this analysis, because the antisymmetrically coupled spin-states no longer have a defined S_T quantum number.

$$\chi_M T = \frac{Ng^2\beta^2}{3k}\left[\frac{\sum S_T(S_T+1)(2S_T+1)\exp\left(-E\{S_T\}/kT\right)}{\sum(2S_T+1)\exp\left(-E\{S_T\}/kT\right)}\right] \quad (14)$$

Table 2 Results of the magnetochemical analysis for **1** and **2**, according to eqns. (4)–(9)

	1	**2**
$g_{\|\|}$ [a]	2.20	2.20
$g_{\perp}$	2.12	2.20
J_{av}/cm^{-1}	−97	−105
δ/cm^{-1}	24	63
G/cm^{-1}	33	47
Δ/cm^{-1}	62	103

[a] Fixed value.

conditions. Second, for both compounds two equally good fits were obtained with $J > J'$ or $J < J'$, but with the same value of J_{av} (eqn. (10)) and the same magnitude of δ.

$$J_{av} = \frac{2J + J'}{3} \qquad (10)$$

This implies that the data cannot distinguish which of the two $S = ½$ states in the spin manifold (Scheme 1) is the lower in energy. Finally, $g_{||}$ and $g_{\perp}$ were also strongly correlated with each other. Hence, $g_{||}$ was fixed to 2.20 in the final fits, in accordance with the EPR data described below.

The refined values of $g_{\perp}$, J_{av}, δ and G from this analysis, and the resultant calculated values of Δ (eqn. (9)), are listed in Table 2. The reproducibility of these parameters in other local minima of the fitting process suggests that their errors can be estimated as: $g = \pm 0.01$, $J_{av} = \delta = G = \pm 2$ cm^{-1} and $\Delta = \pm 3$ cm^{-1}. The fits from eqn. (2) and eqns. (4)–(9) are essentially identical at high temperatures (Fig. 2), and only diverge significantly below 50 K. The values of $g_{\perp}$ and J_{av} from this analysis are also in good agreement with the g and J parameters obtained using eqn. (2) (see above).

As for related $[Cu_3(\mu_3\text{-OH})]^{5+}$ complexes,[2,7,14] the Q-band EPR spectra of **1** and **2** at 290 K are broad and uninformative. Upon cooling to 4 K, however, several features become resolved (Fig. 3). These spectra are similar to that shown by another triangular complex of half-integer S centres showing antisymmetric exchange, whose EPR properties have been interpreted in detail, namely $[Fe_3(\mu_3\text{-O})(\mu\text{-O}_2\text{CMe})_6(OH_2)_3]Cl{\cdot}5H_2O$.§[22] We will discuss the 4 K spectra of **1** and **2** using this earlier treatment. In a weakly axial system (see above) of three antisymmetrically coupled $S = ½$ spins, two strong EPR transitions are expected at moderate magnetic fields at $g_{||}$ and at $g_{\perp}'$, which is related to the true $g_{\perp}$ by eqn. (11).[22]

$$g_{\perp}' = g_{\perp}\left[\frac{\delta^2 - (h\nu)^2}{\Delta^2 - (h\nu)^2}\right]^{1/2} \qquad (11)$$

The two labelled resonances in Fig. 3 correspond to these two parameters in **1** and **2** (Fig. 3). One of these lies near 11 kG, and corresponds to $g_{||} = 2.21$ for **1** or 2.19 for **2**, which are typical $g_{||}$ values for $\{d_{x^2-y^2}\}^1$ or $\{d_{xy}\}^1$ Cu(II) centres.[25] The other lies near 16 kG, at $g_{\perp}' = 1.47$ for **1** or 1.52 for **2**, which are at too high field to be genuine perpendicular components of an isolated $S = ½$ ground state ($g_{\perp} = 2.0$–2.1 would be more typical[25]). The observation of these transitions with $g_{\perp}' << g_e$ confirms that **1** and **2** have isosceles magnetic symmetry or lower (*i.e.* $\delta \neq 0$), that antisymmetric exchange is important to their magnetic structures (*i.e.* $G \neq 0$) and that $\Delta > h\nu$. This is consistent with the magnetochemical analyses, since $h\nu$ for the Q-band EPR experiment is only 1.13 cm^{-1}. Hence, under axial magnetic symmetry eqn. (11) simplifies to eqn. (12):

$$\frac{g_{\perp}'}{g_{\perp}} \approx \frac{\delta}{\Delta} \qquad (12)$$

§ The parameter D referred to in ref. 22 is equivalent to $3^{½}G$ in this paper.

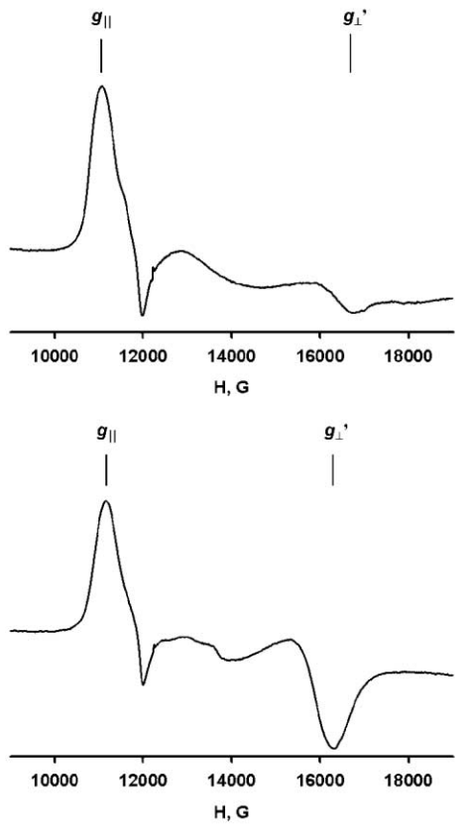

Fig. 3 Q-band EPR spectra at 4 K of powder samples of **1** (top) and **2** (bottom).

Using the values of $g_{\perp}$ derived from the susceptibility analyses, the ratio $g_{\perp}'/g_{\perp} = 0.69$ for both **1** and **2**. By comparison, the susceptibility analysis yields $\delta/\Delta = 0.39(9)$ for **1**, and 0.61(7) for **2**. Hence, it would appear that the assumption of weakly axial magnetic symmetry used to derive eqn. (11), and to model the susceptibility data, is more valid for **2** than for **1**. This is consistent with the different crystallographic symmetries of the $[Cu_3(\mu_3\text{-OMe})]^{5+}$ cores of the complexes, which is effectively axial for **2** but rhombic for **1** (see above).

Two or three other peaks are also present in the EPR spectra of **1** and **2** (Fig. 3): a high-field shoulder on the $g_{||}$ resonance, and one or two peaks at 13–14 kG corresponding to $g_{app} = 1.7$–1.8. Similar, but weaker, features are also shown by $[Fe_3(\mu_3\text{-O})(\mu\text{-O}_2\text{CMe})_6(OH_2)_3]Cl.5H_2O$ at Q-band, but were not assigned.[22] These extra peaks are at inappropriate g-values to arise from a mononuclear impurity in the samples.[25] Rather, they are most likely to be additional transitions from the antisymmetrically coupled $S = ½$ spin states, that become allowed in more strongly axial or rhombic spin environments where $G_x, G_y \neq 0$.[22] In principle, up to six such additional peaks are to be expected. Unfortunately, however, it is not possible to assign these weaker transitions without determining the individual components of the $\boldsymbol{G}$ vector.[22] That would require single crystal EPR experiments, which are outside the scope of this investigation. Nonetheless, it is noteworthy that these extra transitions are more intense in the spectrum of **1** than of **2** (Fig. 3). This is additional evidence that the magnetic structure of **1** in particular is not well described by a model based on weakly axial magnetic symmetry.

The ^{1}H NMR spectra of **1** and **2** in CD_3CN or $(CD_3)_2SO$ show several peaks in the range δ 0–15 ppm, whose integrals do not correspond to simple multiples of each other. In order to probe the solution structures of these compounds further, the partially deuterated species $[Cu_3X(Hpz^{Mes})_2(\mu\text{-}pz^{Mes})_3(\mu_3\text{-OCD}_3)]X$ ($X^- = Cl^-$, d^3-**1**; $X^- = Br^-$, d^3-**2**) were prepared, by carrying out the synthesis of **1** and **2** in CD_3OD. ^{2}H NMR spectra of paramagnetic compounds have much narrower line-

widths than their ^{1}H spectra. Hence, deuteration of a substituent will allow it to be readily detected by ^{2}H NMR, even if it is unobservably broad in the paramagnetic ^{1}H NMR spectrum.[26] The ^{2}H NMR spectra of d^3-**1** and d^3-**2** in CH_3CN were virtually identical, and showed only two peaks of similar integral: at δ,3.6 ppm, which may be assigned to uncomplexed CD_3OH;[27] and at 2.4 ppm, which is of uncertain origin but, given the lack of contact-shifting, is unlikely to correspond to a μ_3-OCD_3 ligand. These data imply that the trinuclear structures of **1** and **2** are not retained in solution. This contrasts with NMR studies on related $[Cu_3(\mu\text{-}L)_3(\mu_3\text{-}OH)]^{2+}$ complexes, which concluded that the triangular core of these compounds retains its structure upon dissolution.[2,7] We propose that steric contacts between the mesityl substituents in **1** and **2** promote ligand dissociation in the donor solvent MeCN.

Conclusions

These data have shown that the products of the reactions of Cu(II) halides with pyrazoles are sensitive to the steric properties of the pyrazole used. The presence of a mesityl, rather than a *tert*-butyl,[1] substituent on the pyrazole proligand results in the clean isolation of a completely different product from these reactions. Compounds **1** and **2** are new variants of a known structural type, with a triply bridging methoxide rather than hydroxide, ligand. A full study of the effects of steric effects, and of supramolecular templating by different anions, on Cu(II)/pyrazole aggregate formation, will be reported elsewhere.[28]

This study represents only the fifth time that antisymmetric exchange in a triangular complex of half-integer-spin ions has been properly interpreted. In addition, to our knowledge this is the first time that magnetic susceptibility and EPR analyses on an antisymmetrically exchange-coupled system have been combined. The values of δ and G derived in this work are broadly similar to those derived from susceptibility measurements of triazolate-bridged $[Cu_3(\mu\text{-}L^1)_3(\mu_3\text{-}OH)(\mu_3\text{-}SO_4)]_n\cdot 6nH_2O$ and $[Cu_3(OH_2)_3(\mu\text{-}L^2)_3(\mu_3\text{-}OH)][NO_3]_2\cdot H_2O$.† [8] However, a smaller value of $G = 6$ cm^{-1} was measured from susceptibility data of $[Cu_3(\mu\text{-}L^3)_3(\mu_3\text{-}OH)]SO_4\cdot 10.5H_2O$,[21,23] while EPR analyses of $[Fe_3(\mu_3\text{-}O)(\mu\text{-}O_2CMe)_6(OH_2)_3]Cl\cdot 5H_2O$ [22] and $[Cr_3(\mu_3\text{-}O)(\mu\text{-}O_2CEt)_6(OH_2)_3]NO_3\cdot 2H_2O$ [29] yielded $G = 1.4$ and 0.62 cm^{-1} respectively. A few measured G values are also available for compounds with other nuclearities or cluster geometries. Antisymmetric exchange has been invoked to explain the magnetic properties of $[Cu_4(\mu_3\text{-}O)(\mu\text{-}Cl)_6(OPPh_3)_4]$,[30] although others have modelled magnetic[31] or EPR [32] data from this or related tetracopper compounds without incorporating it. Mössbauer measurements have yielded values of $G = 0.4$–2.2 cm^{-1} for a series of dinuclear and trinuclear Fe(III) biosites [33,34] and a dinuclear model compound.[33] Finally, susceptibility measurements on two high-nuclearity oxomolybdates, containing embedded hexanuclear V^{IV} centres, yielded $G = 5$–9 cm^{-1}.[35] Although G for **1** and **2** is rather higher than most of these literature values, it is of the order of magnitude predicted by eqn. (13),[36] which yields $G \approx 14$–20 cm^{-1} using $g_{\|}$ values from the EPR spectra, and $g_{\perp}$ from the susceptibility analyses.

$$|G| \approx \left(\frac{\Delta g}{2.0023}\right)|2J_{av}| \qquad (13)$$

where Δg is the deviation of the isotropic g value of the compound from 2.0023. Others have also noted that eqn. (13) tends to underestimate experimentally determined values of G.[22] Unfortunately, data from such a small number of diverse compounds as those listed above, are insufficient to be able to draw conclusions about the magnetostructural factors determining G.

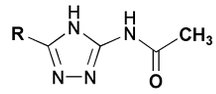

R = H, HL^1
R = NH_2, HL^2

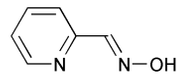

HL^3

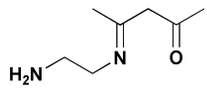

HL^4

Interestingly, the low-temperature EPR spectra of **1** and **2** are notably different from those reported for other $[Cu_3(\mu_3\text{-}OH)]^{5+}$ antisymmetric exchange effects in their low-temperature susceptibility behaviour.[7,14] One series of compounds, $[Cu_3X(OH_2)_2(\mu\text{-}L^1)_3(\mu_3\text{-}OH)]X$ ($X^- = NO_3^-$, $CF_3SO_3^-$ or ClO_4^-), exhibits EPR spectra at 77 K that are typical of an isolated $S = ½$ ground state.[7] The other compound, $[Cu_3(\mu\text{-}L^4)_3(\mu_3\text{-}OH)][ClO_4]_2$ shows more complex EPR spectra at 30 K, but whose main features still lie at g values that are normal for $S = ½$Cu(II) centres.[14] Unfortunately G was not measured for these compounds, so that it is unclear why the EPR spectra in this study should differ so greatly from these other systems. We are presently preparing more triangular complexes of Cu(II) and other $S = ½$ transition ions, to further delineate their magnetochemical and spectroscopic properties.

Experimental

All reactions were carried out in air, while analytical-grade solvents and reagents were used without further purification. 3{5}-(2,4,6-Trimethylphenyl)pyrazole (Hpz^{Mes}) was prepared by the literature method.[16]

Synthesis of $[Cu_3Cl(Hpz^{Mes})_2(\mu\text{-}pz^{Mes})_3(\mu_3\text{-}OCH_3)]Cl$ (1)

Solutions of $CuCl_2$ (0.13 g, 1.0 mmol) in CH_3OH (20 cm^3), and of Hpz^{Mes} (0.37 g, 2.0 mmol) and NaOH (0.040 g, 1.0 mmol) in CH_3OH (30 cm^3), were mixed at 290 K, immediately yielding a dark green precipitate. The mixture was stirred for 16 h, and the precipitate was collected and washed with MeOH. This solid was redissolved in the minimum amount of CH_2Cl_2, and the solution layered with pentane to afford dark green crystals. Yield 0.17 g, 41%. Found C, 60.0; H, 5.8; N, 11.7%: calcd. for $C_{61}H_{70}Cl_2Cu_3N_{10}O$ C, 60.0; H, 5.8; N, 11.5%. An analogous reaction performed in CD_3OD yielded $[Cu_3Cl(Hpz^{Mes})_2(\mu\text{-}pz^{Mes})_3(\mu_3\text{-}OCD_3)]Cl$ (d^3-**1**). Found C, 59.7; H, 5.9; N, 11.7%; calcd. for $C_{61}H_{67}D_3Cl_2Cu_3N_{10}O$ C, 59.9; H, 6.0; N, 11.8%.

Synthesis of $[Cu_3Br(Hpz^{Mes})_2(\mu\text{-}pz^{Mes})_3(\mu_3\text{-}OCH_3)]Br$ (2)

Method as for **1**, using $CuBr_2$ (0.22 g, 1.0 mmol). The product formed dark green crystals from CH_2Cl_2/pentane. Yield 0.26 g, 60%. Found C, 56.1; H, 5.4; N, 10.7%: calcd. for $C_{61}H_{70}Br_2Cu_3N_{10}O$ C, 55.9; H, 5.4; N, 10.7%. An analogous reaction performed in CD_3OD yielded $[Cu_3Br(Hpz^{Mes})_2(\mu\text{-}pz^{Mes})_3(\mu_3\text{-}OCD_3)]Br$ (d^3-**2**). Found C, 56.3; H, 5.6; N, 10.9%; calcd. for $C_{61}H_{67}D_3Br_2Cu_3N_{10}O$ C, 55.8; H, 5.6; N, 10.7%.

Crystal structure determinations

Single crystals of **1** and **2** were grown from CH_2Cl_2/pentane. Experimental details from the structure determinations are given in Table 3. Data were collected using a Nonius KappaCCD area detector diffractometer fitted with an Oxford cryosystems low-temperature device. Both structures were solved by direct methods (SHELXS 97[37]) and refined by full matrix least-squares on F^2 (SHELXL 97[38]). No disorder was detected during refinement of either structure, and no restraints were applied. All non-H atoms were refined anisotropically,

Table 3 Experimental details for the single crystal structure determinations in this study

	1	2
Formula	$C_{61}H_{70}Cl_2Cu_3N_{10}O$	$C_{61}H_{70}Br_2Cu_3N_{10}O$
M_r	1220.79	1309.71
Crystal system	Monoclinic	Orthorhombic
Space group	*Cc*	$Pna2_1$
a/Å	27.2768(3)	22.5523(2)
b/Å	11.4386(2)	11.3697(1)
c/Å	22.8724(3)	23.3653(2)
β/°	122.8131(7)	—
V/Å^3	5997.72(15)	5991.16(9)
Z	4	4
μ/mm^{-1}	1.192	2.438
T/K	150(2)	150(2)
Measured reflections	51189	103098
Independent reflections	13208	13732
R_{int}	0.067	0.100
$R(F)^a$	0.043	0.035
$wR(F^2)^b$	0.114	0.081
Flack parameter	−0.011(8)	−0.003(5)

^{a} $R = \Sigma[|F_o| - |F_c|]/\Sigma|F_o|$ ^{b} $wR = [\Sigma w(F_o^2 - F_c^2)/\Sigma wF_o^4]^{1/2}$.

while all H atoms were placed in calculated positions and refined using a riding model.

CCDC reference numbers 211596 and 211597.

See http://www.rsc.org/suppdata/dt/b3/b311980g/ for crystallographic data in CIF or other electronic format.

Other measurements

Elemental microanalyses were performed by the University of Leeds Department of Chemistry microanalytical service. NMR spectra were obtained on Bruker ARX250 (^{1}H, 250.1 MHz) and DRX500 (^{2}H, 76.8 MHz) spectrometers. EPR spectra were obtained using a Bruker ESP300E spectrometer fitted with an ER5106QT resonator and ER4118VT cryostat. Magnetic susceptibility measurements were performed on a Quantum Design SQUID magnetometer, in an applied field of 1000 G. A diamagnetic correction for the sample was estimated from Pascal's constants;[19] a diamagnetic correction for the sample holder was also applied. The data were refined to eqns. (2) and (3) using SIGMAPLOT.[39] Eqn. (4) was solved in the coupled-spins representation, in which it can be made block-diagonal. The blocks were independently diagonalised using MAPLE[40] (with the RACAH package for angular momentum algebra),[41] leading to analytical equations for the energies of their eigenstates and their derivatives. These expressions were used in a non-linear fit of the van Vleck equation to $\chi_M T$, using an iterative procedure based on the Marquadt method.[42] No paramagnetic impurity or TIP term was included in any of the magnetic analyses.

Acknowledgements

The authors would like to thank Dr H. J. Blythe [University of Sheffield (UK)] for the magnetic susceptibility measurements. Funding by The Royal Society (M.A.H.), the EPSRC (X.L.) and the University of Leeds is gratefully acknowledged.

References

1 X. Liu, J. A. McAllister, M. P. de Miranda, B. J. Whitaker, C. A. Kilner, M. Thornton-Pett and M. A. Halcrow, *Angew. Chem., Int. Ed.*, 2002, **41**, 756.
2 F. B. Hulsbergen, R. W. M. ten Hoedt, G. C. Verschoor, J. Reedijk and A. L. Spek, *J. Chem. Soc., Dalton Trans.*, 1983, 539.
3 M. Angaroni, G. A. Ardizzoia, T. Beringhelli, G. La Monica, D. Gatteschi, N. Masciocchi and M. Moret, *J. Chem. Soc., Dalton Trans.*, 1990, 3305.
4 K. Sakai, Y. Yamada, T. Tsubomura, M. Yabuki and M. Yamaguchi, *Inorg. Chem.*, 1996, **35**, 542.
5 P. A. Angaridis, P. Baran, R. Boca, F. Cervantes-Lee, W. Haase, G. Mezei, R. G. Raptis and R. Werner, *Inorg. Chem.*, 2002, **41**, 2219.
6 A. V. Virovets, N. V. Podberezskaya and L. G. Lavrenova, *J. Struct. Chem.*, 1997, **38**, 440.
7 S. Ferrer, J. G. Haasnoot, J. Reedijk, E. Müller, M. B. Cingi, M. Lanfranchi, A. M. M. Lanfredi and J. Ribas, *Inorg. Chem.*, 2000, **39**, 1859.
8 S. Ferrer, F. Lloret, I. Bertomeu, G. Alzuet, J. Borrás, S. García-Granda, M. Liu-González and J. G. Haasnoot, *Inorg. Chem.*, 2002, **41**, 5821.
9 R. Beckett, R. Colton, B. F. Hoskins, R. L. Martin and D. G. Vince, *Aust. J. Chem.*, 1969, **22**, 2527; B. F. Hoskins and D. G. Vince, *Aust. J. Chem.*, 1972, **25**, 2039; R. Beckett and B. F. Hoskins, *J. Chem. Soc., Dalton Trans.*, 1972, 291.
10 P. F. Ross, R. K. Murmann and E. O. Schlemper, *Acta Crystallogr., Sect. B*, 1974, **30**, 1120.
11 S. Baral and A. Chakravorty, *Inorg. Chim. Acta*, 1980, **39**, 1.
12 R. J. Butcher, C. J. O'Connor and E. Sinn, *Inorg. Chem.*, 1981, **20**, 537.
13 Y. Agnus, R. Louis, B. Metz, C. Boudon, J. P. Gisselbrecht and M. Gross, *Inorg. Chem.*, 1991, **30**, 3155.
14 J. P. Costes, F. Dahan and J. P. Laurent, *Inorg. Chem.*, 1986, **25**, 413.
15 M. Kwiatowski, E. Kwiatowski, A. Olechnowicz, D. M. Ho and E. Deutsch, *Inorg. Chim. Acta*, 1988, **150**, 65.
16 A. L. Rheingold, C. B. White and S. Trofimenko, *Inorg. Chem.*, 1993, **32**, 3471.
17 X. Liu, C. A. Kilner and M. A. Halcrow, *Acta Crystallogr., Sect. C*, 2003, **59**, m100.
18 A. W. Addison, T. N. Rao, J. Reedijk, J. van Rijn and G. C. Verschoor, *J. Chem. Soc., Dalton Trans.*, 1984, 1349.
19 C. J. O'Connor, *Prog. Inorg. Chem.*, 1982, **29**, 203.
20 K. Kambe, *J. Phys. Soc. Jpn.*, 1950, **5**, 48.
21 B. S. Tsukerblat, B. Ya. Kuyavskaya, M. I. Belinskii, A. V. Ablov, N. M. Novotortsev and V. T. Kalinnikov, *Theor. Chim. Acta*, 1975, **38**, 131.
22 Yu. V. Rakitin, Yu. V. Yablokov and V. V. Zelentsov, *J. Magn. Reson.*, 1981, **43**, 288.
23 B. S. Tsukerblat, M. I. Belinskii and V. E. Fainzil'berg, *Sov. Sci. Rev. B: Chem.*, 1987, **9**, 339.
24 M. Gerloch, *Magnetism and Ligand Field Analysis*, Cambridge University Press, Cambridge, UK, 1983.
25 B. A. Goodman and J. B. Raynor, *Adv. Inorg. Chem.*, 1970, **13**, 135.
26 See *e.g.* M. A. Halcrow, J.-S. Sun, J. C. Huffman and G. Christou, *Inorg. Chem.*, 1995, **34**, 4167.
27 D. H. Williams and I. Fleming, *Spectroscopic Methods in Organic Chemistry*, McGraw Hill, London, UK, 5th edn., 1995.
28 X. Liu, J. A. McAllister, M. P. de Miranda, E. J. L. McInnes, C. A. Kilner and M. A. Halcrow, *Chem. Eur. J.*, submitted for publication.
29 H. Nishimura and M. Date, *Bull. Phys. Soc. Jpn.*, 1985, **54**, 395.
30 M. E. Lines, A. P. Ginsberg and R. L. Martin, *Phys. Rev. Lett.*, 1972, **28**, 684.
31 A. B. Blake, C. E. Anson, S. K. arapKoske, R. D. Cannon, U. A. Jayasooriya, A. K. Saad, R. P. White and D. Summerfield, *J. Chem. Soc., Dalton Trans.*, 1997, 2039.
32 T. D. Black, R. S. Rubins, D. K. De, R. C. Dickinson and W. A. Baker jr., *J. Chem. Phys.*, 1984, **80**, 4620.
33 K. E. Kaufmann, C. V. Popescu, Y. Dong, J. D. Lipscomb, L. Que jr. and E. Münck, *J. Am. Chem. Soc.*, 1998, **120**, 8739.
34 Y. Sanakis, A. L. Macedo, I. Moura, J. J. G. Moura, V. Papaefthymiou and E. Münck, *J. Am. Chem. Soc.*, 2000, **122**, 11855.
35 D. Gatteschi, R. Sessoli, W. Plass, A. Müller, A. Krickemeyer, J. Meyer, D. Sölter and P. Adler, *Inorg. Chem.*, 1996, **35**, 1926.
36 T. Moriya, *Phys. Rev.*, 1960, **120**, 91.
37 G. M. Sheldrick, *Acta Crystallogr., Sect. A*, 1990, **46**, 467.
38 G. M. Sheldrick, SHELXL-97, Program for refinement of crystal structures, University of Göttingen, Germany, 1997.
39 SIGMAPLOT (v. 8.02), Program for Tabulating, Modelling and Displaying Data, SPSS Inc., Chicago, USA, 2002.
40 MAPLE 8, Program for the Manipulation of Symbolic Algebra, Waterloo Maple Inc., Waterloo, Canada, 2002.
41 S. Fritzsche, T. Inghoff, T. Bastug and M. Tomaselli, *Comput. Phys. Commun.*, 2001, **139**, 314.
42 W. H. Press, S. A. Teukolsky, W. T. Vetterling and B. P. Flannery, *Numerical Recipes: the Art of Scientific Computing*, Cambridge University Press, Cambridge, UK, 1992.
43 S. Ferrer and F. Lloret, personal communication.